

# Integrated instrumentation for combined polarized single-crystal XAS and diffraction data acquisition for biological applications

Matthew J. Latimer, Kazuki Ito, Scott E. McPhillips and Britt Hedman\*

Stanford Synchrotron Radiation Laboratory, Stanford University, SLAC, 2575 Sand Hill Road, MS 69, Menlo Park, CA 94025, USA. E-mail: hedman@ssrl.slac.stanford.edu

Single-crystal X-ray absorption spectroscopy (XAS) instrumentation, allowing sequential integrated XAS and crystallographic data acquisition during the same experiment and on the same beamline, has been developed for SSRL beamline 9-3, a wiggler side station dedicated to general user biological XAS. The implementation includes a Huber kappa goniometer, Canberra 30-element Ge detector for XAS data collection, open-flow LHe and LN<sub>2</sub> crystal coolers, a microscope for crystal alignment in the beam, and a MarCCD crystallography detector. The kappa goniometer allows a large accessible angular range with an open geometry, affording access to detectors and open stream coolers, as well as future instrumentation. Applicable standard hardware on SSRL crystallography beamlines has been incorporated, with crystallographic data collection controlled *via* the Blu-Ice software developed by the SSRL SMB macromolecular crystallography group. XAS data collection is handled through the SSRL standard XAS-Collect software. Initial diffraction and XAS data from single crystals using an open-flow cryostat are presented. The instrument will be available to general users after the SPEAR3 upgrade in 2004, and future expansion for use in high-throughput structural genomics XAS is proposed.

© 2005 International Union of Crystallography  
Printed in Great Britain – all rights reserved

**Keywords:** single-crystal XAS; EXAFS; polarization; diffraction.

## 1. Introduction

X-ray absorption spectroscopy (XAS) is a very useful tool in structural biology, providing element-specific local structural and electronic information about metal-containing macromolecules in either crystal or solution form (Koningsberger & Prins, 1988). Most biological XAS is performed on frozen solutions resulting in an isotropic spectrum from which oxidation state and symmetry information, and distances to nearest neighbors, can be extracted. The X-ray absorption near-edge structure (XANES region; within ~50 eV of the edge) provides information about oxidation state and symmetry around the absorbing atom (Stöhr, 1992) while the extended X-ray absorption fine structure (EXAFS; ~50–1000 eV beyond the edge) provides precise distance information (typically  $\pm 0.02$  Å for near neighbors,  $< 5$  Å away), along with coordination numbers (within ~25%) and chemical identity of neighbors (to within one row of the periodic table). The information content of the XAS spectrum is limited, however, and, when there is a variety of neighboring atoms at a range of distances, a unique fit to the EXAFS data can be elusive.

One way to enhance the information content of XAS is to utilize polarized spectra of specifically oriented single crystals.

By aligning the absorber–scatterer molecular vector along the direction of X-ray beam polarization, the amplitude of the EXAFS signal can be enhanced for that interaction with an approximate  $\cos^2\theta$  dependence (Penner-Hahn & Hodgson, 1986). Similarly, delineating information about electronic structure can be elucidated from the XANES through the polarization dependence of the electronic transitions (Hahn *et al.*, 1982; Smith *et al.*, 1985; Tyson *et al.*, 1989; Brouder, 1990; Shadle *et al.*, 1993; Pickering & George, 1995). The enhanced information content of polarized XAS spectra from single crystals is obtained at the cost of increased complexity of the experimental apparatus, data collection and analysis. Although several studies on biological systems have been published (Bianconi *et al.*, 1985; Penner-Hahn & Hodgson, 1986; Flank *et al.*, 1986; Chen *et al.*, 1993; Shadle *et al.*, 1993), the number is far smaller than that of published isotropic XAS solution studies and probably reflects the inherent difficulties of measuring and analyzing polarized data.

Previous studies at SSRL and elsewhere have been generally hampered by the inability to adjust and verify crystal/interatomic vector orientations *in situ* while measuring on an XAS beamline, or by the lack of optimized XAS data-collection software and necessary fluorescence detectors on crystallography beamlines. The approach described here is to

make the single-crystal XAS measurements easily accessible for both crystallographers and X-ray spectroscopists, and to perform both techniques on the same specimen. Hence, two experimental set-ups (XAS and crystallography) have been merged, such that experienced users in either technique have the same tools they know and expect for the familiar part of the experiment, and easy access to the tools necessary for the less known part of the experiment. At the current stage of implementation, users need bring only frozen crystals on standard crystallography mounting pins and can start collecting data with virtually no set-up time.

In addition to experimental equipment in the hutch, polarized single-crystal experiments also require synchrotron beamlines with relatively high X-ray flux as well as a small beam size. A brief description of SSRL beamline 9-3 optics and performance is provided below, as it is an integral part of the overall performance of the instrumentation and experiment.

## 2. SSRL beamline 9-3

SSRL beamline 9-3 is a side station on the 16-pole, 2 T wiggler beamline 9 and is dedicated to general user biological XAS. The beamline operates over an energy range of approximately 5–35 keV and the optics are designed to provide a high-flux focused beam across a range of energy where most biologically interesting metals absorb ( $\sim 5$ –13 keV). The focus spot in the hutch ( $\sim 0.7$  mm  $\times$  4 mm FWHM) is limited by the large horizontal source size, a result of the off-axis positioning of a side station on a wiggler, and is not expected to change very significantly with the SPEAR3 upgrade. For the results described below, a 500  $\mu$ m  $\times$  500  $\mu$ m beam was used, resulting in  $\sim 4 \times 10^{10}$  photons  $s^{-1}$  delivered to the sample at 7100 eV.

The beamline optics (see Fig. 1) consist of a dual mirror system where the initial element ( $M_0$ ) is a 1 m flat bent water-cooled Rh-coated silicon mirror providing harmonic rejection, power filtering and vertical collimation before the monochromator. The  $M_0$  mirror eliminates the need to detune the monochromator for harmonic rejection and the collimation provides excellent energy resolution with the full beam. The second mirror ( $M_1$ ) is a cylindrical bent Rh-coated Xerodur mirror placed after the monochromator to provide vertical and horizontal focusing into the experimental hutch. The monochromator is an in-vacuum liquid-nitrogen-cooled double-crystal design (Rowen *et al.*, 2001) with two sets of Si(220) crystal pairs (two different azimuthal orientations of the 220 planes) that can be brought in and out of the beam without warming and breaking vacuum. Si(220) crystals were chosen for both energy range and resolution, with the two different orientations provided to allow avoidance of crystal glitches for specific energy ranges/elements.

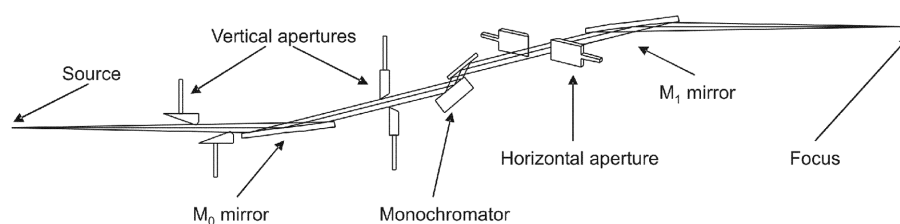


**Figure 1**  
Schematic diagram of the optical elements of SSRL BL9-3.

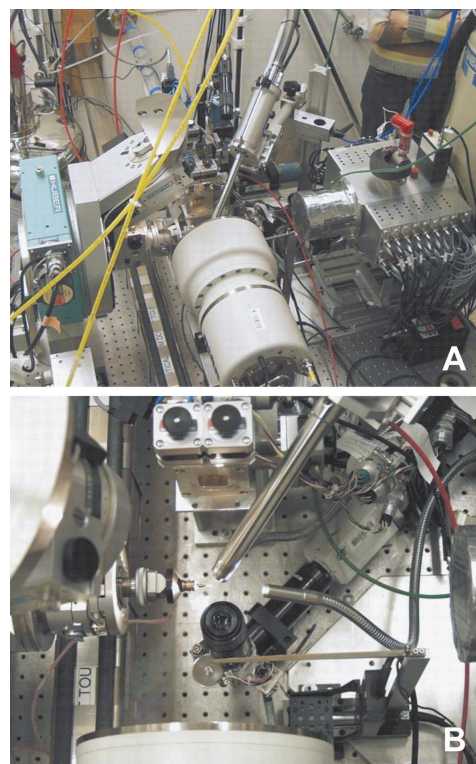


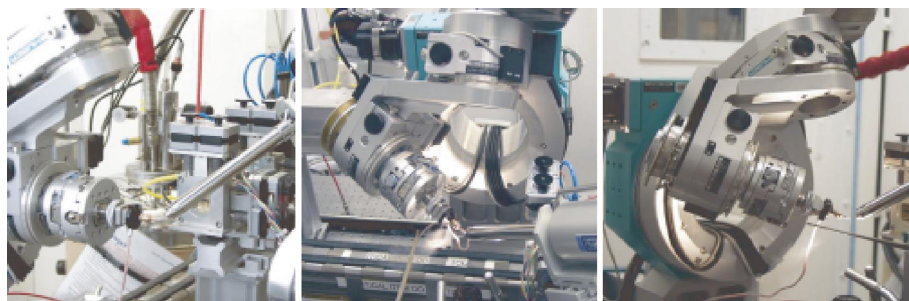
**Figure 2**  
Overviews of the experimental apparatus. A: overall arrangement of hardware with the XAS fluorescence detector on the right, kappa goniometer on the left, crystal cooler on the upper right, and MarCCD crystallography detector in the foreground. B: arrangement of hardware around the sample with the microscope directly below and the crystal cooler coming in from the upper right.

## 3. Instrumentation

The motivation for creating a combined XAS and diffraction instrument on SSRL BL9-3 was to provide easy access to all the necessary tools for complete measurements of biological macromolecular crystals using both techniques on a single beamline. As much as possible, existing elements of the standard crystallography and XAS beamline hardware were used both to maximize the familiarity of the set-up for regular users of either technique, and to provide ready availability of spares. An overview of the instrumentation is given in Fig. 2 and descriptions of each component are given below.

### 3.1. $I_0$ section

The  $I_0$  section consists of a 10 cm active-length ion chamber with two sets of motorized slits, the first set (Huber 3013) to


**Figure 3**

Three views demonstrating the flexibility of the kappa goniometer in the experimental set-up. The presence of the end-station beamline 9-2 transport pipe (visible at the bottom of the middle picture) limits motions below the level of the X-ray beam but the entire arc above is essentially free of interference.

define the entering beam and the second (JJ X-ray) to minimize the scatter from the exiting beam just before the sample. A home-built pneumatic shutter assembly is incorporated between the ion chamber and the scatter slits. This shutter is an important part of the experiment set-up, controlling diffraction data exposure times for the MarCCD detector, and for XAS data acquisition, closing during each move to XAS scan data points and during the monochromator re-wind between scans, under the current stepping-motor set-up. In a typical 20 min XAS scan, ~25% of the time represents monochromator motion, which for samples that are subject to photoreduction is a significant exposure. Use of the shutter results in a significant improvement of crystal lifetime.

### 3.2. Kappa goniometer

The instrument is based around a Huber kappa goniometer (model 515.2) for crystal mounting, alignment and diffraction measurements. It is mounted on low-profile Thompson rails, which enables it to be easily slid in/out of place for specific set-ups. The BL9-3 experimental hutch has a pseudo-end-station configuration with access on both sides of the beam, and with the BL9-2 end-station beam pipe traversing the top of the experimental table. The open geometry of the kappa goniometer (Fig. 3) allows for access of the detectors, cooling, microscope and future external equipment, such as lasers or optical spectroscopy instruments. Unlike most diffraction measurements, single-crystal XAS requires that the crystal lattice be positioned precisely at specific orientations relative to the polarization vector of the X-ray beam; thus the flexibility of the kappa goniometer is a key element and well worth the calculational complexity of kappa *versus* Eulerian geometry. Despite geometrical constraints imposed by the BL9-2 end-station pipe and other surrounding equipment, it is perceived that with the flexible set-up of the modular instrument it would be a rare event not being able to reach a specific orientation. A motorized X-Y-Z positioning stage on the goniometer head represents a second important element, allowing fast alignment of the crystal in the cold stream and precise positioning at the goniometer focus point. The goniometer head incorporates a standard SSRL/SMB-designed heated shield to prevent icing.

### 3.3. MarCCD detector

Diffraction data are recorded with a MarCCD 165 detector (Mar USA), which has a  $4k \times 4k$  chip bonded to a fiber optic taper and gives a  $\sim 80 \mu\text{m}$  pixel size with a detector active-area diameter of 165 mm. The image distortion and uniformity of response of the detector are corrected in the data-acquisition software. The detector is mounted on a motorized stage (Velmex BiSlide) for translation along the beam direction. The MarCCD is protected from direct beam using a motorized (two axes) tungsten beam

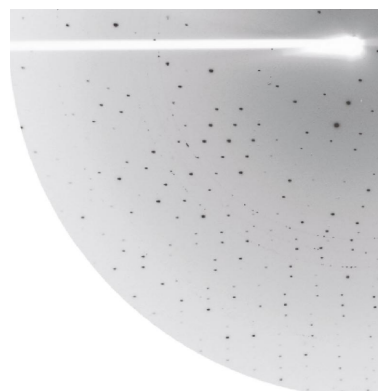
stop with an integrated photodiode for alignment and monitoring of the X-ray beam (Ellis *et al.*, 2003). A diffraction pattern from an initial experiment is shown in Fig. 4 and, although there is significant background scattering, indexing the crystal was easily accomplished. Background sources of scatter have since been significantly reduced.

### 3.4. Ge detector

XAS data are measured in fluorescence mode using a 30-element solid-state Ge detector array (Canberra, GL0055S) equipped with analog processing electronics (Canberra, 2016). Multichannel analyzer (MCA) functions and setting of single-channel analyzer (SCA) discriminators are handled through the Canberra Instrument Control Bus (ICB) and Ethernet-accessible Acquisition Interface Modules (Canberra, 556A) and associated Canberra software. This system allows SCA discriminator control and MCA trace inspection *via* an SSRL-developed software interface optimized for ease of use with multi-element detectors and XAS experiments. The Ge detector is mounted on a motorized slide for remote positioning relative to the sample to optimize count-rate levels.

### 3.5. Crystal cooling

Two open-flow cooling systems are available for use on BL9-3 with the single-crystal instrumentation. An Oxford


**Figure 4**

A single quadrant of a MarCCD diffraction image from recombinant P6 myoglobin collected at 13 keV/0.954 Å.

Instruments Cryojet is available for temperatures to  $\sim 100$  K. All single-crystal XAS data obtained to date have been measured using this Oxford Cryojet, or on pre-aligned crystals inserted into the BL9-3 standard Oxford Instruments CF-1208 enclosed liquid-helium (LHe) cryostat usually used for solution XAS. A LHe open-flow cooler from Cryo Industries (HFC-1645 LHe-Cryocool) has recently been acquired, which will allow sample temperature control to as low as  $\sim 10$  K. The lower temperature of the LHe cooler is desirable for both reduction of vibrational disorder and for slowing down the rate of photoreduction of the metal centers. Lower temperatures are particularly important for XAS data collection, which is, in many cases, performed at lower energy than crystallographic studies, and where therefore larger absorption coefficients result in an increased photoreduction rate.

### 3.6. Microscope

Alignment of the crystal on the goniometer head is facilitated by the use of a Navitar 12X zoom-lens system with a motorized zoom attached to a 1/2" format color CCD camera (JAI CV-S3200) and mounted directly below the crystal. At maximum zoom the horizontal field of view is  $\sim 0.6$  mm with the system as a whole providing a good range of magnification, allowing both rough and fine alignments with a  $\sim 10$  cm working distance that provides access space around the crystal for other components of the instrument. The system also maintains focus throughout the zoom range and can be adjusted to give a constant center point throughout the range. A loop-mounted myoglobin crystal is shown in Fig. 5 at three stages of magnification. Images are displayed on screens inside and outside the hutch, are captured using a standalone Axis network video server (Axis Communications, 2400), and can be displayed *via* a web interface as well as stored to media.

### 4. Data-collection software

The data collection for the two parts of the experiment, diffraction and XAS, is controlled by two different sets of programs on different computing platforms. Control of the goniometer and the shutter is shared between the two computer systems and is easily switched back and forth. For each type of data collection, the software that the user encounters is identical to that used for either diffraction or XAS alone at other SSRL beamlines.

Diffraction data are collected using the SSRL-developed Blu-Ice interface and Distributed Control System (DCS)



**Figure 5**

Three views at different magnifications of a  $\sim 0.2$  mm  $\times$  0.2 mm loop-mounted crystal using the Navitar microscope.

software running on Linux/UNIX and used on all SSRL macromolecular crystallography beamlines (McPhillips *et al.*, 2002). The MarCCD detector is accessed by Blu-Ice/DCS through a TCP/IP socket connection to a dedicated PC running Linux and functioning as a remote server controlling the MarCCD.

XAS data collection is handled by SSRL standard VMS-based XAS-Collect software (George, 2000), which is optimized for ease of use for XAS experiments and which incorporates control of the X-ray shutter into XAS scans to minimize X-ray exposure.

### 5. Results

As a test of the integrated instrument, full diffraction and XAS data sets were collected on the same crystal of recombinant P6 myoglobin [Sigma M-7257, crystallization as in Cohen *et al.* (2001)]. A  $\sim 300$   $\mu\text{m} \times 200$   $\mu\text{m} \times 200$   $\mu\text{m}$  single crystal was mounted in a fiber loop, dipped in a cryoprotectant solution of 25% sucrose in mother liquor, then quickly frozen in liquid nitrogen. The crystal was thereafter mounted on the goniometer into a nitrogen coldstream at 100 K. Diffraction data were first collected at an energy/wavelength of 13 keV/0.954  $\text{\AA}$  (Fig. 4) suitable for crystallographic data collection, after which XAS data were collected at the Fe *K* edge. For the data presented here, 18 scans (15 min each) were averaged to give the edge and EXAFS spectra presented in Fig. 6. The edge spectrum of even a single scan was sufficient to identify the transition features on the rising edge and monitor photoreduction, and the averaged edge is of very high quality, clearly showing subtle features and resolvable pre-edge structure. The isolated  $k^3$ -weighted EXAFS data are presented in Fig. 6(b) and show high-quality data appropriate for analysis to  $k \simeq 14$   $\text{\AA}^{-1}$ .

The time required to switch between diffraction and XAS data collection was  $< 5$  min.

### 6. Conclusion and future developments

An instrument for performing both diffraction and XAS measurements on standard biological samples prepared for crystallography has been designed and implemented on a high-flux focused wiggler beamline. The combined instrumentation has been constructed such that crystallographers and spectroscopists encounter the software and equipment familiar to them for their respective experiments and easy access to the tools necessary for each other's experiments. Initial experiments have demonstrated that the integrated system works well, providing good-quality diffraction and XAS data from protein single crystals with negligible time required to switch between diffraction and spectroscopy data acquisition, which are performed sequentially.

The next stage in this development is to create software tools that allow the user to easily predict the optimum angular position for data collection of polarized XAS of known structures. Also, the LHe cooler will be integrated into the setup and additional standard features of SSRL crystallography

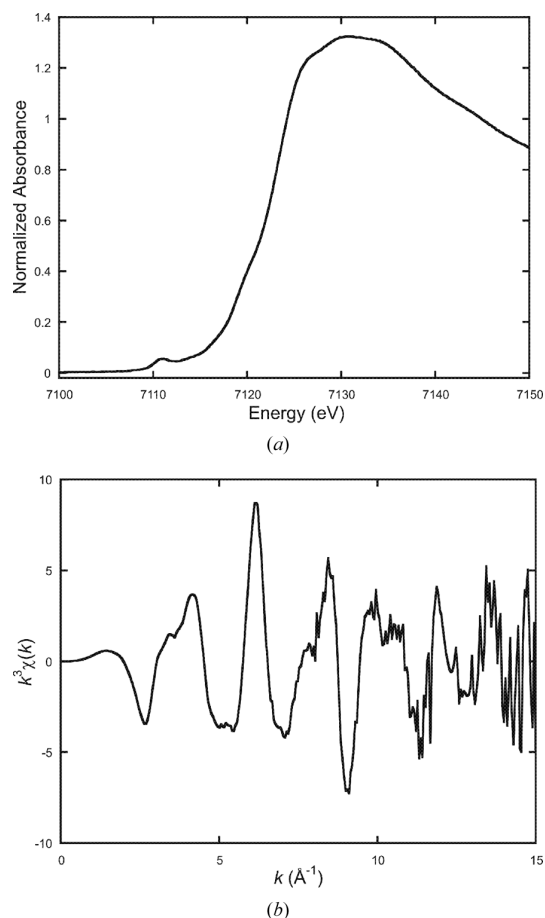


**Figure 6**  
Fe  $K$ -edge absorption edge (a) and EXAFS (b) of a single crystal of recombinant P6 myoglobin.

beamlines will be incorporated, *i.e.* automated crystal alignment.

The use of standard diffraction apparatus and tools also allows for the future expansion to take advantage of the developments in automation that have been made for high-throughput crystallography at SSRL (Cohen *et al.*, 2002) and their application in an analogous way to high-throughput XAS measurements. Through the use of robotic sample changers and loop-mounted samples, large numbers of crystals could be quickly scanned for metal content and appropriate edge spectra collected. In addition, high-throughput XAS measurements need not be limited to crystals, but could also be performed on solutions frozen in loops, allowing measurements to be made of a wider range of samples, including those that do not crystallize.

The authors thank many of the members of the SSRL SMB program staff for help with hardware, software and crystallographic techniques, especially T. M. McPhillips, A. Gonzalez, P. J. Ellis, A. E. Cohen and T. Eriksson in the crystallography group. The developments and data collection were performed at SSRL, a national user facility operated by Stanford University on behalf of the US Department of Energy, Office of Basic Energy Sciences. The instrument development was funded within the SSRL Structural Molecular Biology Program, which is supported by the National Institutes of Health, National Center for Research Resources, Biomedical Technology Program, and the Department of Energy, Office of Biological and Environmental Research.

## References

- Bianconi, A., Congiu-Castellano, A., Durham, P. J., Hasnain, S. S. & Phillips, S. (1985). *Nature (London)*, **318**, 685–687.
- Brouder, C. (1990). *J. Phys. Condens. Matter*, **2**, 701–738.
- Chen, J., Christiansen, J., Campobosso, N., Bolin, J. T., Tittsworth, R. C., Hales, B. J., Rehr, J. J. & Cramer, S. P. (1993). *Angew. Chem. Int. Ed.* **32**, 1592–1594.
- Cohen, A., Ellis, P., Kresge, N. & Soltis, S. M. (2001). *Acta Cryst.* **D57**, 233–238.
- Cohen, A. E., Ellis, P. J., Miller, M. D., Deacon, A. M. & Phizackerley, R. P. (2002). *J. Appl. Cryst.* **35**, 720–726.
- Ellis, P. J., Cohen, A. E. & Soltis, S. M. (2003). *J. Synchrotron Rad.* **10**, 287–288.
- Flank, A. M., Weiniger, M., Mortenson, L. E. & Cramer, S. P. (1986). *J. Am. Chem. Soc.* **108**, 1049–1055.
- George, M. J. (2000). *J. Synchrotron Rad.* **7**, 283–286.
- Hahn, J. E., Scott, R. A., Hodgson, K. O., Doniach, S., Desjardins, S. R. & Solomon, E. I. (1982). *Chem. Phys. Lett.* **88**, 595–598.
- Koningsberger, D. C. & Prins, R. (1988). *X-ray Absorption Spectroscopy*. New York: Wiley.
- McPhillips, T. M., McPhillips, S. E., Chiu, H.-J., Cohen, A. E., Deacon, A. M., Ellis, P. J., Garman, E., Gonzalez, A., Sauter, N. K., Phizackerley, R. P., Soltis, S. M. & Kuhn, P. (2002). *J. Synchrotron Rad.* **9**, 401–406.
- Penner-Hahn, J. E. & Hodgson, K. O. (1986). *Structural Biological Applications of X-ray Absorption, Scattering and Diffraction*, edited by H. D. Bartunik and B. Chance, pp. 35–47. New York: Academic Press.
- Pickering, I. J. & George, G. N. (1995). *Inorg. Chem.* **34**, 3142–3152.
- Rowen, M., Peck, J. W. & Rabedeau, T. (2001). *Nucl. Instrum. Methods*, **A467**, 400–403.
- Shadle, S. E., Penner-Hahn, J. E., Schugar, H. J., Hedman, B., Hodgson, K. O. & Solomon, E. I. (1993). *J. Am. Chem. Soc.* **115**, 767–776.
- Smith, T. A., Penner-Hahn, J. E., Berding, M. A., Doniach, S. & Hodgson, K. O. (1985). *J. Am. Chem. Soc.* **107**, 5945–5955.
- Stöhr, J. (1992). *NEXAFS Spectroscopy*. Berlin: Springer Verlag.
- Tyson, T. A., Roe, A. L., Frank, P., Hodgson, K. O. & Hedman, B. (1989). *Phys. Rev. B*, **39**, 6305–6315.